coatings

MDPI

Article

Microstructure and Wear Resistance of AlCoCrFeNiTi High-Entropy Alloy Coatings Produced by HVOF

Martin Löbel *, Thomas Lindner, Thomas Mehner and Thomas Lampke

Materials and Surface Engineering Group, Institute of Materials Science and Engineering, Chemnitz University of Technology, D-09125 Chemnitz, Germany; th.lindner@mb.tu-chemnitz.de (T.Li.); thomas.mehner@mb.tu-chemnitz.de (T.M.); thomas.lampke@mb.tu-chemnitz.de (T.La.)

* Correspondence: martin.loebel@mb.tu-chemnitz.de; Tel.: +49-371-531-31865

Received: 28 July 2017; Accepted: 5 September 2017; Published: 12 September 2017

Abstract: The investigation of high-entropy alloys (HEAs) has revealed many promising properties. HEAs with a high share of Al and Ti are suitable for the formation of lightweight materials. Investigations of the alloy system AlCoCrFeNiTi showed high strength, hardness, ductility, and wear resistance, which makes this special alloy interesting for surface engineering and particularly for thermal spray technology. In this study, the suitability of inert gas-atomised HEA powder for high-velocity-oxygen-fuel (HVOF) thermal spray is investigated. This process allows for high particle velocities and comparatively low process temperatures, resulting in dense coatings with a low oxidation. The microstructure and phase composition of the atomised powder and the HVOF coating were investigated, as well as the wear behaviour under various conditions. A multiphase microstructure was revealed for the powder and coating, whereas a chemically ordered bcc phase occurred as the main phase. The thermal spray process resulted in a slightly changed lattice parameter of the main phase and an additional phase. In comparison with a hard chrome-plated sample, an increase in wear resistance was achieved. Furthermore, no brittle behaviour occurred under abrasive load in the scratch test. The investigation of wear tracks showed only minor cracking and spallation under maximum load.

Keywords: HEA; high-entropy alloy; CCA; compositionally complex alloy; thermal spray; HVOF; phase composition; microstructure

1. Introduction

High-entropy alloys (HEAs) are a new class of multicomponent alloy systems. They are typically composed of at least five elements with approximately equimolar amounts [1]. Several alloys have been investigated which showed the capability of forming multicomponent solid solutions with a simple fcc and bcc structure without brittle and intermetallic phases. Cantor et al. proved the existence of one single fcc phase in the equimolar alloy CoCrFeMnNi [2]. HEAs exhibit several outstanding properties, including high hardness, strength, ductility, wear, and corrosion resistance [3–5]. However, many previous investigations have shown that most alloy systems are composed of several phases, partially including complex phases. Therefore, the term "compositionally complex alloys" (CCAs) was introduced for alloys which consist of at least two phases [6].

One alloy system which has been studied in detail is AlCoCrCuFeNi and the copper-free alloy system AlCoCrFeNi [7,8]. Additional alloying has been investigated in this system for the further improvement of material properties. Due to its large atomic radius, titanium showed a strong influence on mechanical properties, leading to solid solution strengthening. However, the formation of intermetallic phases was observed for high titanium contents [9–13]. Investigations of the influence of alloying elements also showed a large effect of aluminium content on phase composition and

mechanical properties. A high content of aluminium promotes the formation of bcc phases [14,15]. Detailed investigations revealed that aluminium stabilises a chemically ordered bcc phase with B2 structure. Furthermore, the increase of aluminium content suppresses the formation of a centred cluster (cc) with A12 structure type [16]. The investigation of the equimolar alloy AlCoCrFeNiTi showed a dendritic structure consisting of two bcc solid solutions and good mechanical properties in compression tests, including high fracture strength and plastic strain [17]. Moreover, the wear behaviour of this alloy system was investigated for bulk samples, showing promising wear resistance in comparison with the conventional steels SUJ2 (EN 1.3505) and SKH51 (EN 1.3343) [11,18].

Due to their high strength and wear resistance, HEAs and CCAs are promising candidates to be applied for surface technologies (e.g., thermal spray), to achieve a functional division between substrate and surface. This approach can help to save costs and resources, as HEAs and CCAs usually contain expensive and rare alloying elements such as cobalt. First investigations to produce HEA/CCA coatings by thermal spray have already been carried out [19–21].

For the equimolar alloy AlCoCrFeNiTi, the suitability of different powder production routes for atmospheric plasma spray (APS) was investigated. The production route of inert gas atomisation proved to be most suitable for the fabrication of spherical and homogeneous alloyed powder. Relatively homogeneous and wear-resistant coatings can be produced by applying this powder for APS. However, APS coatings produced with atomised powder showed distinct porosity and oxide lamella. Furthermore, brittle coating behaviour occurred under abrasive load in scratch tests, where spallation and secondary cracks appeared [19].

One approach to improving coating properties is the application of other thermal spray processes. The high-velocity-oxygen-fuel (HVOF) spray process is characterised by high particle velocity (supersonic particle jet) and a comparatively low process temperature. These process characteristics result in coatings with a high bonding strength, as well as a low porosity and oxide content [22].

The focus of this study is the fabrication of wear-resistant equimolar AlCoCrFeNiTi coatings by applying atomised powder for HVOF spray process. Wear behaviour is investigated under different wear conditions and compared with a hard chrome-plated sample.

2. Materials and Methods

Powder material of the alloy system AlCoCrFeNiTi with equimolar composition was produced as feedstock by inert gas atomisation. In a first step, the alloying elements were melted under vacuum to produce a homogeneous alloy. The alloy was subsequently atomised using argon as a process gas to avoid impurities and reactions. In the next step, the powder was sieved to a grain size of −63 +20 µm in a Retsch AS 200 sieve tower (Retsch Technology GmbH, Haan, Germany).

The particle size distribution was examined by laser diffraction analysis in a Cilas 930 device (Cilas, Orléans, France). Metallographic cross-sections of the powder were prepared by standard metallographic procedures and investigated in a scanning electron microscope (SEM) LEO 1455VP (Zeiss, Jena, Germany) with an acceleration voltage of 25 kV. A backscattered electron detector (BSD) was used to visualise material contrast by different grey levels. The analysis of the chemical composition was performed by energy dispersive X-ray spectroscopy (EDS) (GENESIS, EDAX, Mahwah, NJ, USA). Furthermore, phase analysis was conducted by X-ray diffraction (XRD) with a D8 Discover diffractometer from Bruker AXS (Billerica, MA, USA) using Co Kα radiation with a tube voltage of 40 kV and a tube current of 40 mA. The diffractograms were measured in a diffraction angle range (2θ) of 10° to 130° with a step size of 0.01° and 1.5 s/step. Due to the use of a 1D Lynxeye XE detector, this value corresponds to 288 s/step. The powder diffraction file (PDF) database 2014 was applied for phase identification.

Coating was performed on flat steel (S235) substrates with a diameter of 40 mm. The samples were pretreated by corundum blasting with abrasive grain size of −600 +425 µm, a pressure of 3.5 bar, and a distance of 100 mm at an angle of 60°. The uncoated samples were subsequently cleaned in an ultrasonic bath with ethanol. The coating process was conducted with a liquid-fuelled HVOF K2

system (GTV Verschleissschutz GmbH, Luckenbach, Germany). Parameter studies were carried out to optimise porosity and hardness. The optimum parameters mentioned in Table 1 were applied to coat samples for extensive investigation of microstructure and wear behaviour.

Table 1. Optimised high-velocity-oxygen-fuel (HVOF) coating parameters.

O_2	Kerosin	N_2	Powder Feed Rate	No. of Layers	Spray Distance	Relative Traverse Speed	Spray Path Offset	Nozzle Length
810 L/min	22.5 L/h	11 L/min	80 g/min	9	360 mm	70 m/min	5 mm	100 mm

After the coating process, samples were ground in an industrial flat grinding process. Cross-sections of the coating were prepared by standard metallographic procedures and investigated in SEM. The chemical composition was examined by EDS, and phase analysis was conducted by XRD. Furthermore, the microhardness (Vickers hardness HV 0.1) was measured in metallographic cross-sections with a Wilson Tukon 1102 device (Buehler, Uzwil, Switzerland). The average value and standard deviation was calculated from ten single indents.

After microstructural investigations, the wear behaviour was studied under different tribological conditions in ball-on-disk, oscillating wear, and scratch tests. All wear tests were carried out under controlled conditions in air at a temperature of 22 ± 2 °C and a humidity of 50 ± 10%. Different wear tests were carried out to investigate the wear behaviour under adhesive, oscillating, and abrasive wear conditions. Therefore, a Tetra Basalt Tester (Tetra, Ilmenau, Germany), a Wazau SVT 40 device (Wazau, Berlin, Germany) and a CSM Revetest-RST device (CSM Instruments SA, Peseux, Switzerland) were used with the parameters summarised in Table 2.

Table 2. Wear test parameters.

Ball-On-Disk Test		Oscillating Wear Test		Scratch Test	
Force	20 N	Force	26 N	Mode	progressive
Radius	5 mm	Frequency	40 Hz	Force	1–200 N
Speed	96 RPM	Time	900 s	Speed	2.5 mm/min
Cycles	15916	Amplitude	0.5 mm	Length	5 mm
Counter body	Al_2O_3	Counter body	Al_2O_3	Tip	truncated diamond cone
Diameter	6 mm	Diameter	10 mm	Radius	200 µm

As a reference, a hard chrome-plated sample deposited in an industrial process was investigated. The measurement of surface hardness revealed a value of 885 ± 54 HV 0.1. All wear marks were analysed by laser scanning microscopy (LSM) with a Keyence VK-X200 device (Keyence, Osaka, Japan) to determine the resulting wear depth. Furthermore, wear marks of the scratch test were investigated in SEM.

3. Results and Discussion

3.1. Feedstock Characterisation

The microstructure of the atomised and sieved AlCoCrFeNiTi powder was investigated in powder cross-sections in SEM. To determine the particle size distribution, a laser diffraction analysis was carried out. The results of the feedstock characterisation are shown in Figure 1.

The powder particles have a predominantly spherical shape and exhibit a homogeneous microstructure. Two phases can be distinguished within the particles. Despite sieving the powder to remove very fine particles with a particle size of under 20 µm, smaller particles still exist in the powder. The results of the particle size analysis shown in Figure 1b reveal a mean particle size (d50) of 25 µm and a particle size range (−d90 +d10) of −58 +9 µm. Furthermore, particle size analysis shows that there was a fraction of very fine particles with a size of under 20 µm in the powder, which is

in accordance with microscopic analysis. The preparation of powder by sieving was not sufficient to remove all very fine particles, whereas coarse particles could be removed.

Phase analysis of the feedstock was conducted by XRD. The resulting diffractogram is shown in Figure 2.

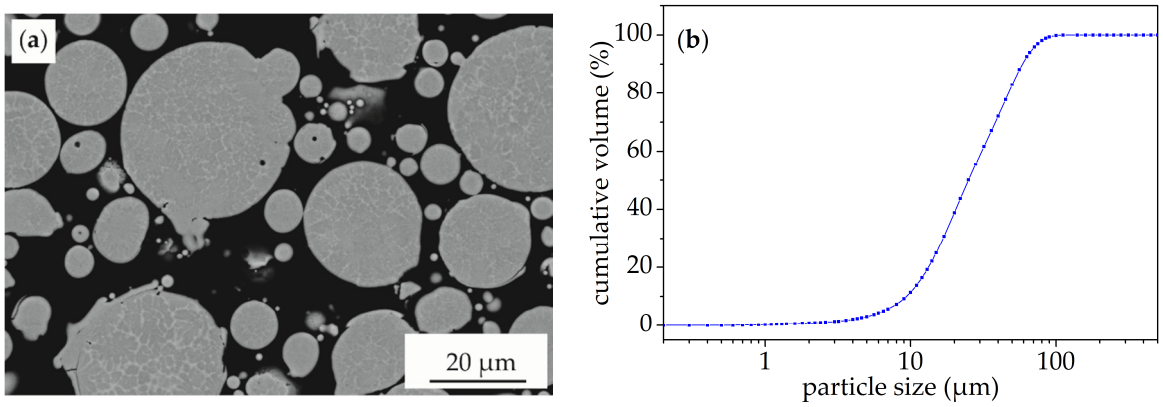

Figure 1. Results of feedstock characterisation: (**a**) SEM (backscattered electron detector, BSD) images of powder cross-sections; (**b**) Cumulative particle size distribution (volume).

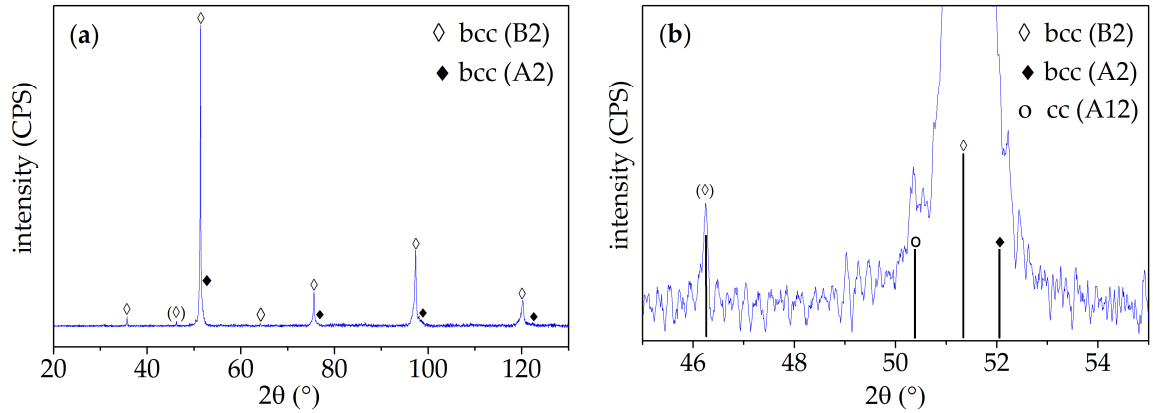

Figure 2. XRD pattern of atomised and sieved powder: (**a**) Overview; (**b**) Detailed view of the main peak of the bcc (B2) phase.

The diffraction peaks with the highest intensity can be ascribed to a bcc (B2) phase. However, some of these peaks exhibit a shoulder towards higher diffraction angles. In Figure 2b, an enlarged view in the 2θ range of 45°–55° is depicted, showing the asymmetric shape of the peak and the overlapping with the peak of a bcc (A2) phase. The atomised powder contains a minor content of this phase. Investigations of different particle size fractions of atomised powder with similar composition revealed that the peaks of the bcc (A2) phase were more distinct for coarse particle size fractions, indicating higher phase content. For small particles (which are cooled down faster in the atomisation process), the formation of the bcc (A2) phase was mostly suppressed. Furthermore, two more peaks are present in the enlarged area of the diffraction pattern. The diffraction peak at 50.4° can be attributed to the cc (A12) phase, which has been detected in arc-melted samples of the same alloy system [16]. The diffraction pattern indicates that small amounts of this phase were present in the atomised powder. Another peak appears at 46.2°, which is the main diffraction peak of the bcc (B2) phase due to the presence of and interaction with low-intensity Co Kβ radiation.

3.2. Coating Characterisation

Cross-sections of the coatings were prepared and investigated in a SEM with a BSD to visualise material contrast by different grey levels. Images of the coating are shown in Figure 3.

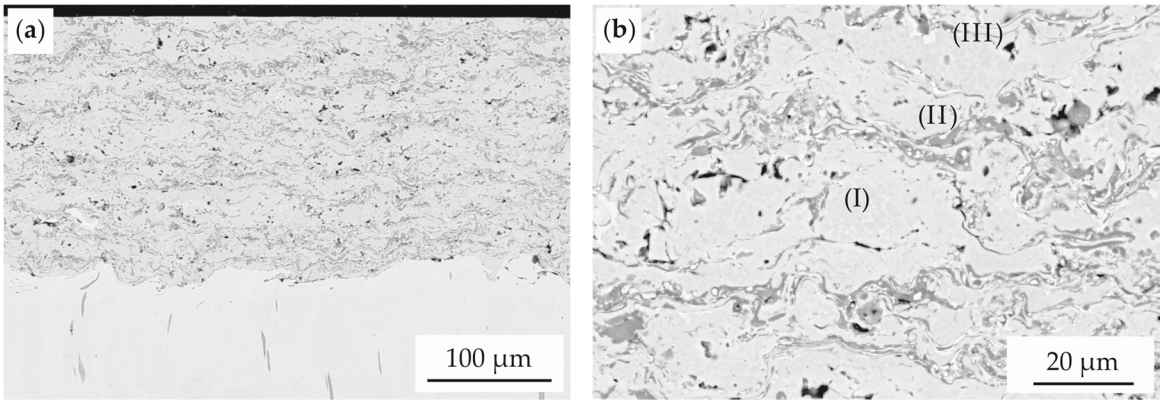

Figure 3. SEM images (BSD detector) of HVOF-sprayed AlCoCrFeNiTi coating: (**a**) Overview; (**b**) In detail with (I) spray particle, (II) oxide lamella and (III) pore.

The images show a lamellar and homogeneous coating structure. A coating thickness of approximately 210 µm was measured for the coating after the flat grinding process. In Figure 3b, with higher magnification, several phases can be distinguished in the coating, which is in accordance with the feedstock analysis. However, the coating exhibits distinct oxide lamella and pores. The formation of oxide lamella might be caused by the high content of very fine powder particles, which are more reactive due to their high specific surface area.

The overall composition of the feedstock and coating was measured by EDS. Due to the equimolar composition, each alloying element has a nominal value of 16.7 at.%. The results are shown in Table 3.

Table 3. Chemical composition of atomised AlCoCrFeNiTi powder and HVOF coating in at.%, measured by energy dispersive X-ray spectroscopy (EDS).

Sample	Atomised Powder	HVOF Coating
Al	18.6	18.7
Co	16.2	16.3
Cr	16.2	15.8
Fe	16.4	16.6
Ni	16.4	16.4
Ti	16.2	16.1

The chemical composition of the atomised powder is in good accordance with the nominal composition. Only the aluminium content showed a distinct deviation of over 1 at.%. After the thermal spray process, the chemical composition of the coating only showed a minor deviation below 0.5 at.% in comparison to the atomised powder.

According to powder characterisation, phase analysis was carried out by XRD. The resulting diffractogram is shown in Figure 4.

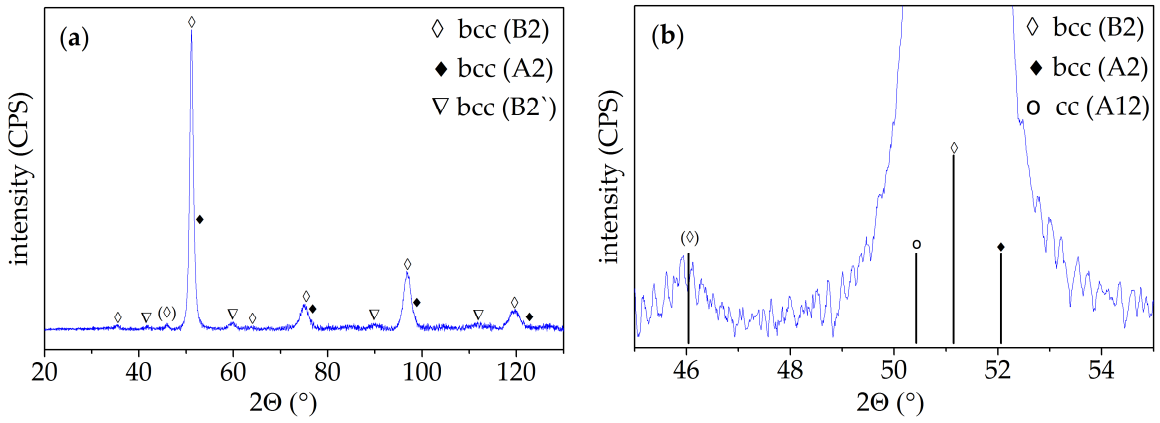

Figure 4. XRD pattern of HVOF-sprayed AlCoCrFeNiTi coating: (**a**) Overview; (**b**) Detailed view of the main peak of the bcc (B2) phase.

The XRD pattern of the HVOF-sprayed coating exhibits high intensity diffraction peaks, which are slightly shifted to lower diffraction angles compared to the atomised powder. According to phase analysis for atomised powder, these diffraction peaks can be ascribed to a bcc (B2) phase. Evaluation shows that the lattice parameter increased from 2.92 to 2.93 Å. For samples produced with arc-melting, a lattice parameter of 2.94 Å was determined for the bcc (B2) phase, showing that phase formation sensitively depends on the cooling conditions [16]. Compared to the feedstock material, a widening of the high-intensity diffraction peaks occurred. The widening of the diffraction peaks might be caused by inhomogeneous cooling conditions in the thermal spray process due to a variation of powder particle size. Fine powder particles are cooled down very quickly, resulting in fine coating grain sizes. The widening of the main peaks resulted in the overlapping with the low-intensity peaks of the bcc (A2) phase. Due to the widening of the high-intensity diffraction peak of the bcc (B2) phase, no distinct peak of the bcc (A2) phase could be observed in the 2θ range of 45°–55°. The overlapping also occurred for the diffraction peak of the cc (A12) phase. Similar to powder analysis, a bcc (B2) peak of the low-intensity Co Kβ radiation appears at 46°, which is slightly shifted. In comparison with feedstock material, peaks of an additional phase appear, which can be referred to as another bcc (B2) phase with a lattice parameter of 3.58 Å. The formation of this additional phase needs to be investigated in further studies. No distinct and assignable peaks of oxide phases appeared. A summary of all phases detected in the powder and HVOF coating is stated in Table 4.

Table 4. Summary of phases detected by XRD in equimolar AlCoCrFeNiTi atomised powder and HVOF coating. Due to the overlapping of the diffraction peaks of the main B2 phase, the lattice parameters of the A2 and A12 phases could not be determined in the coating.

Sample	Struktur-Bericht	Lattice	Structure Type	Pearson Symbol	Space Group	Lattice Parameter (Å)
powder	B2	bcc	CsCl	cP2	$Pm\bar{3}m$ (221)	2.92
	A2	bcc	W	cI2	$Im\bar{3}m$ (229)	2.88
	A12	cc	α-Mn	cI58	$I\bar{4}3m$ (217)	8.91
coating	B2	bcc	CsCl	cP2	$Pm\bar{3}m$ (221)	2.93
	B2	bcc	CsCl	cP2	$Pm\bar{3}m$ (221)	3.58
	A2	bcc	W	cI2	$Im\bar{3}m$ (229)	–
	A12	cc	α-Mn	cI58	$I\bar{4}3m$ (217)	–

For the HVOF-sprayed coating, a microhardness of 730 ± 82 HV 0.1 was determined. In comparison to APS-sprayed coatings of the same alloy produced with atomised feedstock, a distinct increase of hardness can be achieved [19].

The results of the wear tests carried out under various wear conditions are shown in Figure 5.

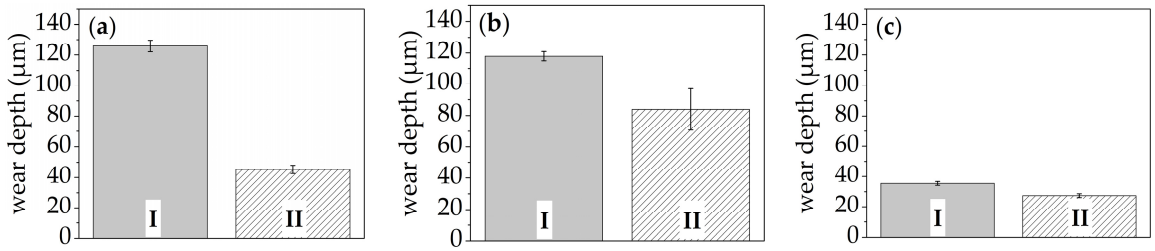

Figure 5. Wear depth of the reference hard chrome-plated sample (I) and HVOF sprayed coatings (II) in: (**a**) Ball-on-disk; (**b**) Oscillating wear; and (**c**) Scratch test.

The results of ball-on-disk tests exhibit a lower wear depth for the HVOF-sprayed coating, showing that a higher wear resistance could be achieved compared to a hard chrome-plated sample. The investigations under oscillating wear conditions showed the same tendency. Furthermore, under abrasive wear conditions in scratch tests, a slightly lower wear depth was measured for the HVOF-sprayed coating. The wear depth is also distinctly lower compared to the coating of the same alloy produced by APS (atomised powder), showing that the resistance against abrasive wear can be improved by using the HVOF spray process [19]. The wear tracks of the scratch tests were investigated by SEM (BSD). In Figure 6, an image of the surface area where the highest load was applied and an exemplary wear depth profile (LSM) are shown.

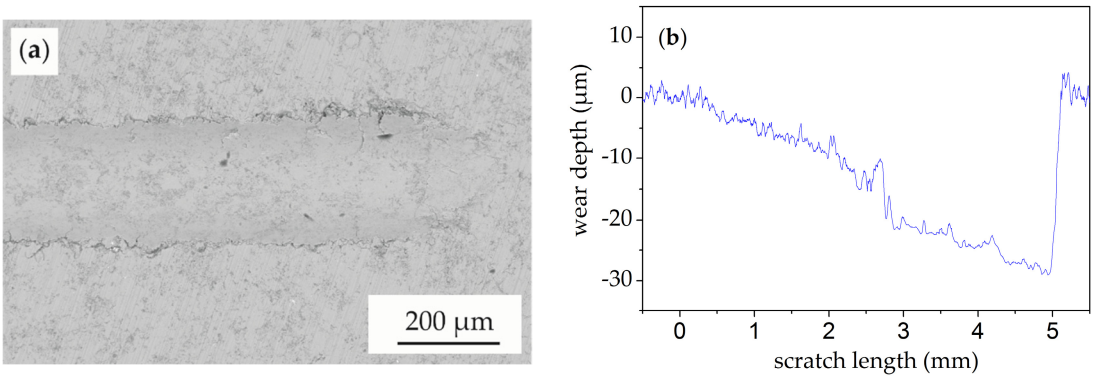

Figure 6. Results of HVOF coating scratch test: (**a**) Coating surface after progressive load scratch test; (**b**) Wear depth profile.

The surface of the HVOF-sprayed coating only shows minor cracks and spallation in the area where the highest load was applied in progressive load scratch tests. In contrast to the coating of the same alloy produced with APS (atomised powder), no brittle failure occurred [19]. The wear depth profile shows a continuous increase of wear depth with increasing scratch length (force).

4. Summary and Conclusions

Atomised powder of the equimolar CCA system AlCoCrFeNiTi has been successfully applied for a HVOF thermal spray process. The investigation of the atomised feedstock material revealed a multiphase structure. A chemically ordered bcc phase with B2 structure occurred as a main phase. Furthermore, a chemically disordered bcc phase with A2 structure and a centred cluster with A12 structure were detected. After the thermal spray process, the phase characteristics have slightly changed. The bcc (B2) phase still appeared as the main phase, whereas the lattice parameter was changed. Furthermore, another bcc B2 phase with a distinctly changed lattice parameter occurred. Microstructural investigations of the coating revealed a homogeneous and lamellar multiphase structure. However, coatings produced with HVOF showed distinct oxide lamella. These are probably

caused by a high content of very fine powder particles, which are more reactive due to their high specific surface. The investigation of particle size distributions showed that sieving is not suitable to remove the majority of fine particles.

For the HVOF coating, a high microhardness of 730 ± 82 HV 0.1 was measured. The wear behaviour of the coatings was investigated under various wear conditions in ball-on-disk, oscillating wear, and scratch tests. In comparison with a hard chrome-plated sample, a higher wear resistance could be achieved by applying CCAs for HVOF. Furthermore, no brittle failure occurred under abrasive load in scratch tests, making CCAs a potential candidate for wear-resistant coatings.

Acknowledgments: The publication costs of this article were funded by the German Research Foundation/DFG and the Technische Universität Chemnitz in the funding programme Open Access Publishing. The authors thank Marc Pügner for conducting the XRD measurements and assistance during their evaluation.

Author Contributions: Martin Löbel and Thomas Lindner conceived and designed the experiments; Martin Löbel, Thomas Lindner and Thomas Mehner performed the experiments, analysed the data and wrote the paper. Thomas Lampke directed the research and contributed to the discussion and interpretation of the results.

Conflicts of Interest: The authors declare no conflict of interest.

References

1. Yeh, J.-W.; Lin, S.-J.; Chin, T.-S.; Gan, J.-Y.; Chen, S.-K.; Shun, T.-T.; Tsau, C.-H.; Chou, S.-Y. Formation of simple crystal structures in Cu-Co-Ni-Cr-Al-Fe-Ti-V alloys with multiprincipal metallic elements. *Metall. Mater. Trans. A* **2004**, *35*, 2533–2536. [CrossRef]
2. Cantor, B.; Chang, I.; Knight, P.; Vincent, A. Microstructural development in equiatomic multicomponent alloys. *Mater. Sci. Eng. A* **2004**, *375–377*, 213–218. [CrossRef]
3. Yeh, J.W. Recent progress in high-entropy alloys. *Ann. Chim. Sci. Mat.* **2006**, *31*, 633–648. [CrossRef]
4. Murty, B.S.; Yeg, J.-W.; Ranganathan, S. *High-Entropy Alloys*; Elsevier: Amsterdam, The Netherlands, 2014.
5. Gao, M.C.; Yeh, J.-W.; Liaw, P.K.; Zhang, Y. *High-Entropy Alloys: Fundamentals and Applications*, 1st ed.; Springer International Publishing: Cham, Switzerland, 2016.
6. Miracle, D.B.; Miller, J.D.; Senkov, O.N.; Woodward, C.; Uchic, M.D.; Tiley, J. Exploration and Development of High Entropy Alloys for Structural Applications. *Entropy* **2014**, *16*, 494–525. [CrossRef]
7. Singh, S.; Wanderka, N.; Murty, B.S.; Glatzel, U.; Banhart, J. Decomposition in multi-component AlCoCrCuFeNi high-entropy alloy. *Acta Mater.* **2011**, *59*, 182–190. [CrossRef]
8. Tsai, M.-H.; Yeh, J.-W. High-Entropy Alloys: A Critical Review. *Mater. Res. Lett.* **2014**, *2*, 107–123. [CrossRef]
9. An, Y.; Hou, G.; Chen, J.; Zhao, X.; Liu, G.; Zhou, H.; Chen, J. Microstructure and tribological properties of iron-based metallic glass coatings prepared by atmospheric plasma spraying. *Vacuum* **2014**, *107*, 132–140. [CrossRef]
10. Chen, M.R.; Lin, S.J.; Yeh, J.W.; Chen, S.K.; Huang, Y.S.; Tu, C.P. Microstructure and Properties of $Al_{0.5}CoCrCuFeNiTi_x$ (x = 0−2.0) High-Entropy Alloys. *Mater. Trans.* **2006**, *47*, 1395–1401. [CrossRef]
11. Chuang, M.-H.; Tsai, M.-H.; Wang, W.-R.; Lin, S.-J.; Yeh, J.-W. Microstructure and wear behavior of $Al_xCo_{1.5}CrFeNi_{1.5}Ti_y$ high-entropy alloys. *Acta Mater.* **2011**, *59*, 6308–6317. [CrossRef]
12. Wang, Y.; Ma, S.; Chen, X.; Shi, J.; Zhang, Y.; Qiao, J. Optimizing mechanical properties of $AlCoCrFeNiTi_x$ high-entropy alloys by tailoring microstructures. *Acta Mater.* **2013**, *26*, 277–284.
13. Yu, Y.; Wang, J.; Li, J.; Kou, H.; Liu, W. Characterization of BCC phases in $AlCoCrFeNiTi_x$ high entropy alloys. *Mater. Lett.* **2015**, *138*, 78–80. [CrossRef]
14. Zhang, K.; Fu, Z. Effects of annealing treatment on phase composition and microstructure of $CoCrFeNiTiAl_x$ high-entropy alloys. *Intermetallics* **2012**, *22*, 24–32. [CrossRef]
15. Li, C.; Li, J.C.; Zhao, M.; Jiang, Q. Effect of aluminum contents on microstructure and properties of $Al_xCoCrFeNi$ alloys: 16th International Symposium on Metastable, Amorphous and Nanostructured Materials. *J. Alloys Compd.* **2010**, *504*, 515–518. [CrossRef]
16. Lindner, T.; Löbel, M.; Mehner, T.; Dietrich, D.; Lampke, T. The Phase Composition and Microstructure of $Al_xCoCrFeNiTi$ Alloys for the Development of High-Entropy Alloy Systems. *Metals* **2017**, *7*, 162. [CrossRef]
17. Zhou, Y.J.; Zhang, Y.; Wang, Y.L.; Chen, G.L. Solid solution alloys of $AlCoCrFeNiTi_x$ with excellent room-temperature mechanical properties. *Appl. Phys. Lett.* **2007**, *90*, 181904. [CrossRef]

18. Yu, Y.; Wang, J.; Li, J.; Kou, H.; Duan, H.; Li, J.; Liu, W. Tribological behavior of AlCoCrCuFeNi and $AlCoCrFeNiTi_{0.5}$ high entropy alloys under hydrogen peroxide solution against different counterparts. *Tribol. Int.* **2015**, *92*, 203–210. [CrossRef]
19. Löbel, M.; Lindner, T.; Kohrt, C.; Lampke, T. Processing of AlCoCrFeNiTi high entropy alloy by atmospheric plasma spraying. *IOP Conf. Ser. Mater. Sci. Eng.* **2017**, *181*, 12015. [CrossRef]
20. Wang, L.-M.; Chen, C.-C.; Yeh, J.W.; Ke, S.-T. The microstructure and strengthening mechanism of thermal spray coating $Ni_xCo_{0.6}Fe_{0.2}Cr_ySi_zAlTi_{0.2}$ high-entropy alloys. *Mater. Chem. Phys.* **2011**, *126*, 880–885. [CrossRef]
21. Ang, A.S.M.; Berndt, C.C.; Sesso, M.L.; Anupam, A.; Praveen, S.; Kottada, R.S.; Murty, B.S. Plasma-Sprayed High Entropy Alloys: Microstructure and Properties of AlCoCrFeNi and MnCoCrFeNi. *Metall. Mater. Trans. A* **2015**, *46*, 791–800. [CrossRef]
22. Tucker, R.C., Jr. *ASM Handbook, Volume 5A: Thermal Spray Technology*; ASM International: Novelty, OH, USA, 2013.